VOL. 17, NO. 16, AUGUST 2022 ISSN 1819-6608
ARPN Journal of Engineering and Applied Sciences

www.arpnjournals.com

ADVANTAGES OF THE EFFECTIVE POTENTIAL IN THE STUDY OF THE OSCILLATION MODES OF THE PHYSICAL SYMMETRIC PENDULUM

José Hernández[1], D. Peña Lara[2, 3] and H. Correa[4]
[1]Departamento de Física, Universidad Popular del Cesar, 200004, Valledupar, Colombia
[2]Grupo de Transiciones de Fase y Materiales Funcionales, Universidad del Valle, Cali, Colombia
[3]Centro de Excelencia en Nuevos Materiales (CENM), Universidad del Valle, Cali, Colombia
[4]Laboratorio de Optoelectrónica, Universidad del Quindío, Armenia, Colombia
E-Mail: diego.pena@correounivalle.edu.co

ABSTRACT

Studies in pendulums (oscillatory motion) are significant in physics, engineering, and other fields of knowledge and continue to be a topic of active research. Considering the Lagrangian formalism and using the technique of variation of canonical variables, the physical symmetrical pendulum was studied. Using the conservation laws, we introduce the effective one-dimensional potential, which depends on the dimensionless variable ζ (related implicit with nutation angle) and parametrically on reduced energy ε and two reduced angular momenta,p_1 and p_2. Only three modes (plane, elliptical, and conical) were studied using the effective potential. An advantage to using this approach was to obtain approximate analytical expressions to study the phase diagrams that show the pendulum's behavior; therefore, in the plane mode, the motion is on a plane, in the elliptical mode, the pendulum moves quasi elliptical, and in the conical mode, the pendulum vibrates at a single point - the three modes depending on the initial condition. An advantage of this approach was to obtain approximate analytical expressions to study the phase diagrams for these three modes. This approach simplifies and visibility a complex problem as the oscillations of the physical pendulum.

Keywords: physical symmetrical pendulum, effective potential, lagrangian formalism, space phase, oscillation modes.

INTRODUCTION

A pendulum is a rigid object (bob) attached to a string, rod, thread, or cord of length ℓ, oscillating freely from a stationary point (pivot). If the string (rod, thread, or cord) is massless, it is commonly known as a simple pendulum. Considering only the rotational motion of the rigid body, we have a mathematical pendulum. Also, taking into consideration the mass of the string (rod, thread, or cord), a physical pendulum (PP) is obtained [1, 2]. Many pendulums proposed are theoretical and have applications in different fields of knowledge, such as torsion, inverted, paraconic, symmetric, Foucault, chaotic, coupled, quantum, among others [3-19].

The dynamics of the spinning symmetric top have been extensively studied [20-24], where the spin motion and apsidal precession are the most important. Considering that the precession and spin motions are small perturbations for a PP, a physical symmetrical pendulum (PSP) with three degrees of freedom is obtained [25], where the nutation motion is dominant. A series of approaches have studied the symmetric top and the PSP problems to describe their dynamics [26, 27].

In this work, we consider the Lagrangian formalism to deduce an effective potential that depends on one variable (ζ) and three fitting parameters (ε, p_1, p_2) to describe the motion of PSP in terms of Euler angles and to analyze the different oscillation modes (plane, elliptical, and conical).

THEORETICAL ASPECTS

Figure1 displays a PSP of mass m and length ℓ, $X\,Y\,Z$ is a local space-fixed inertial coordinate system and $\bar{X}\bar{Y}\bar{Z}$ for the pendulum-fixed. The Euler angles (ϕ, θ, ψ) specify an orientation of the fixed axesand form a set of generalized coordinates. Between ϕ and φ (azimuthal angle of the spherical coordinates), there is a difference of phase of π/2 ($\phi = \varphi + \pi/2$).

The description of the motion of PSP is given in terms of (ϕ, θ, ψ), being ϕ the precession angle, ψ the angle of rotation around $\bar{Z}$ (symmetry axis), and θ the angle between axes $\bar{Z}$ and Zor nutation angle.
The kinetic and the potential energies are:

$$T(\dot{\phi}, \theta, \dot{\theta}, \dot{\psi}) = \frac{1}{2}\left\{I_{\bar{x}}\left[\dot{\theta}^2 + \dot{\phi}^2 \sin^2(\theta)\right] + I_{\bar{z}}\left[\dot{\phi}\cos(\theta) + \dot{\psi}\right]^2\right\} \quad (1)$$

$$V(\theta) = -mg\ell\cos(\theta) \quad (2)$$

where $I_{\bar{n}}, n = x, z$are the momenta of inertia with respect to $\bar{X}$, $\bar{Z}$, respectively.

The Lagrangian of the system is:

$$L(\dot{\phi}, \theta, \dot{\theta}, \dot{\psi}) = T(\dot{\phi}, \theta, \dot{\theta}, \dot{\psi}) - V(\theta) \quad (3)$$

The angles $\phi$and ψ are cyclic coordinates [not appear explicitly in Equation (3)]; therefore, their corresponding angular momenta p_ϕ and p_ψ are constant of motion. Mechanical energy $E = T + V$is also invariant (conserved) and the problem to quadrature is reduced [20].

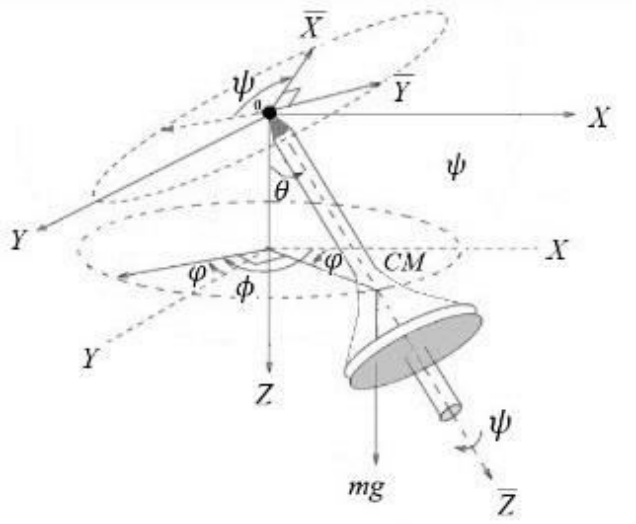

Figure-1. Physical symmetrical pendulum. XYZ are the fixed axes on an inertial reference frame, ϕ, θ,and ψ are the Euler angles used to describe the motion.

The conservation laws are:

$$p_{\phi} = \frac{\partial L}{\partial \dot{\phi}} = I_{\bar{x}}\,\dot{\phi}\sin^2(\theta) + I_{\bar{z}}\cos(\theta)\left[\dot{\psi} + \dot{\phi}\cos(\theta)\right] \quad (4)$$

$$p_{\psi} = \frac{\partial L}{\partial \dot{\psi}} = I_{\bar{z}}\left[\dot{\phi}\cos(\theta) + \dot{\psi}\right] \quad (5)$$

Temporal variation of $\dot{\phi}$ is $\bar{Z}$ -rotation around Z-axis or precession, ψ ($\dot{\psi}$) means pendulum rotation around Z-axis or spin motion, From Equations (4) and (5):

$$\dot{\phi} = \frac{p_{\phi} - p_{\psi}\cos(\theta)}{I_{\bar{x}}\sin^2(\theta)} \quad (6)$$

$$\dot{\psi} = \frac{p_{\psi}}{I_{\bar{z}}} - \dot{\phi}\cos(\theta) \quad (7)$$

E is a quadratic form in canonical variables:

$$E = \frac{1}{2}\left\{I_{\bar{x}}\dot{\theta}^2 + \frac{\left[p_{\psi}\cos(\theta) - p_{\phi}\right]^2}{I_{\bar{x}}\sin^2(\theta)} + \frac{p_{\psi}^2}{I_{\bar{z}}}\right\} - mg\ell\cos(\theta) \quad (8)$$

where the "zero point" of potential energy is at the top of the pendulum.

Let us introduce the following variables:

$$\mathcal{E} = \frac{E}{mg\ell} \;\; ; \;\; P_{\phi,\psi} = \frac{p_{\phi,\psi}}{\sqrt{mg\ell I_{\bar{x}}}} \;\; ; \;\; \alpha = \frac{I_{\bar{x}}}{I_{\bar{z}}} \quad (9)$$

where α is related to the shape of the pendulum and can have three values: $\alpha > 1$(ellipsoid moment of inertia is elongated or prolate), $\alpha < 1$ (ellipsoid moment of inertia is flattened or oblate), and $\alpha = 1$ (spherical ellipsoid), equation(8) becomes

$$\mathcal{E} = \frac{1}{2}\left\{\dot{\theta}^2 + \left[P_{\psi}\cot(\theta) - P_{\phi}\csc(\theta)\right]^2 + \alpha P_{\psi}^2\right\} - \cos(\theta) \quad (10)$$

EFFECTIVE POTENTIAL APPROACH

The dominant force acting upon a PSP is the gravitational force; therefore, the net torque is zero (angular momentum constant) around the central point, the effective potential is introduced to reduce to the equivalent one-dimensional problem [20, 28].

To find an exact analytical solution to the PSP (problem with three degrees of freedom and three constants of motion), one makes evident $\dot{\theta}^2$ from Equation (10):

$$\dot{\theta}^2 = 2\cos(\theta) - \left\{\left[P_{\psi}\cot(\theta) - P_{\phi}\csc(\theta)\right]^2 + \alpha P_{\psi}^2\right\} + 2\mathcal{E} \quad (11)$$

and by using the dimensionless variable,

$$\zeta = \frac{z}{\ell} = \cos(\theta) \quad (12)$$

Equation (11) becomes:

$$\dot{\zeta}^2 = (1-\zeta^2)\left(2\mathcal{E} - \alpha P_{\psi}^2 + 2\zeta\right) - \left(P_{\psi}\zeta - P_{\phi}\right)^2 \quad (13)$$

Based on the new parameters

$$\varepsilon = \mathcal{E} + \frac{1-\alpha}{2}P_{\psi}^2 p_1 = P_{\phi}P_{\psi} \quad (14)$$

Equation (13) becomes

$$\varepsilon = \frac{\dot{\zeta}^2}{2} + V_{\text{eff}}(\zeta; \varepsilon, p_1, p_2) \quad (15)$$

Where

$$V_{\text{eff}}(\zeta; \varepsilon, p_1, p_2) = \zeta^3 + \varepsilon\zeta^2 - (1+p_1)\zeta + p_2^2 \quad (16)$$

is so-called effective potential. $V_{\text{eff}}(\zeta; \varepsilon, p_1, p_2)$ depends on the variable ζ and three constants of motion ε, p_1, and p_2 (physical parameters adjustment). The roots of the cubic polynomial (16) will be interpreted as the turning points.

By minimizing Equation (16), the critical points obtained are:

$$\left.\frac{\partial V_{\text{eff}}(\zeta;\varepsilon,p_1,p_2)}{\partial\zeta}\right|_{\zeta=\bar{\zeta}} = 3\zeta^2 + 2\varepsilon\zeta - (1+p_1) = 0 \quad (17)$$

Varying the initial conditions p_1, p_2, and ε-parameter, the physical criterion for energies is through Equation (17), which has two real solutions:

$$\bar{\zeta}_{\substack{\max\\\min}} = -\frac{1}{3}\left[\varepsilon \pm \sqrt{\varepsilon^2 + 3(1+p_1)}\right] \quad (18)$$

due to ζ-axis being in the direction of the gravitational field, $\bar{\zeta}_{\max} < 0$ and $\bar{\zeta}_{\min} > 0$. These points depend on energy and their momenta concerning $\phi$and ψ.

Evaluating the effective potential (16) at the values (18), one gets

$$V_{\text{eff}}\left(\bar{\zeta}_{\substack{\max\\\min}};\varepsilon,p_1,p_2\right)=\varepsilon_{\substack{\max\\\min}} \quad (19)$$

with

$$\varepsilon_{\substack{\max\\\min}}=\frac{1}{27}\left[27p_2^2+9(1+p_1)\varepsilon+2\varepsilon^3\pm(6+6p_1+2\varepsilon^2)\sqrt{3+3p_1+\varepsilon^2}\right] \quad (20)$$

here, $\varepsilon_{\max}$ and $\varepsilon_{\min}$ are not upper bounds, but functions depend on thetotal energy of the system. From Equations (20), one obtains the conditions (physically accepted) that must impose onε, p_1, and , p_2 to characterize the system.

RESULTS AND DISCUSSIONS

For the case with reduced energy $\varepsilon = 0.4$, reduced momenta $p_1 = 1$, and $p_2 = 1$, the PSP has an asymmetric motion as plotted in Figure-2 (solid line represents the behavior of effective potential V_{eff} as a function of ζ). The critical points, projected on the ζ-axis are labeled by$\bar{\zeta}_{\max} = -0.9606$ and$\bar{\zeta}_{\min} = 0.6939$, according to Equation (18).

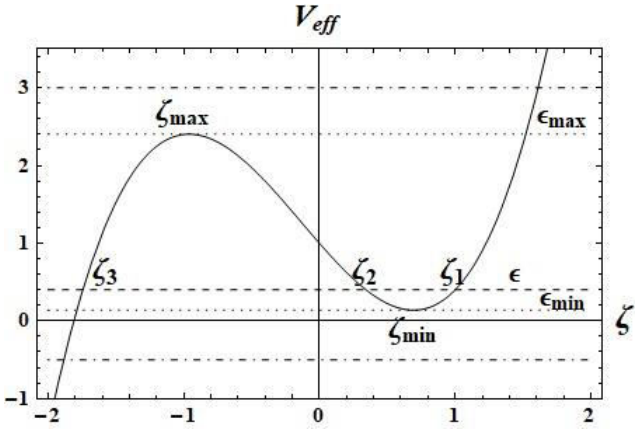

Figure-2. The asymmetric behavior of ζ-dependence of effective potential V_{eff}. The two horizontal dotted lines indicate the values of $V_{\text{eff}}(\bar{\zeta}_{\max};\varepsilon,p_1,p_2)$ and $V_{eff}(\bar{\zeta}_{min};\varepsilon,p_1,p_2)$with $\bar{\zeta}_{\max} = -0.9606$ and $\bar{\zeta}_{\min} = 0.6939$. The dashed line represents the physical solution for $\varepsilon = 0.4$, withinitial conditions $p_1 = 1$ and $p_2 = 1$. The two dash-dotted lines mean unphysical solutions.

The two horizontal dotted lines indicate the values of $V_{\text{eff}}(\bar{\zeta}_{\max};\varepsilon,p_1,p_2) = 2.4039$ and $V_{\text{eff}}(\bar{\zeta}_{\min};\varepsilon,p_1,p_2) = 0.1389$, according to Equations (20), respectively. The points labeled byζ_i,i = 1, 2,3 are the turning points, in other words, the pendulum has an oscillatory motion between these two points. The dashed line represents an acceptable physical condition (with a determined reduced energyε). The dash-dotted line represents the unphysical solutions.

From Figure-2, in order to have the motion always bounded in the region of physical interest, the parameters meet the following conditions:

$$0\le\bar{\zeta}_{\min}\le 1;\quad -1\le\bar{\zeta}_{\max}\le 0;\quad \varepsilon_{\min}\le\varepsilon\le\varepsilon_{\max} \quad (21)$$

where $\varepsilon_{\max/\min}$ does not mean upper/lower bounds but relative maximum/minimum points, respectively. The first two conditions of (21) are reduced to:

$$-1\le p_1\le 2\qquad \tfrac{1}{2}(p_1-2)\le\varepsilon\le\tfrac{1}{2}(2-p_1) \quad (22)$$

For energies $\varepsilon>\varepsilon_{\max}or\varepsilon<\varepsilon_{\min}$, we have unphysically solutions (there are no turning points) as shown by the dash-dotted lines corresponding to$\varepsilon = 0.5$ and 3.0 in Figure-2.

Oscillation Modes

In the phase space or space of all possible states (positions and their momenta), we will focus on the three oscillation modes: plane, conical, and elliptical. These modes depend on the value given to the reduced energy and reduced angular momenta.

From the experimental point of view, $P_{\phi,\psi}$is minus two orders of magnitude and $p_1$about minus four, and $\cos(\theta)\approx 1$. Therefore, the precession and the spin motion will besmall perturbations to the representative nutation motion.

Plane Mode

If the center of mass (CM) of the PSP is released near the surface of the Earth under the following initial conditions: from a starting position ($\theta=\theta_0$) and zero transverse speed ($\dot{\phi}=0$), from Equation (6), we have:

$$P_\phi = P_\psi\cos(\theta)\equiv P_\psi\zeta \quad (23)$$

Equation (13) becomes:

$$\dot{\zeta}^2=-2(\zeta^3+\varepsilon\zeta^2-\zeta+p_2^2-\varepsilon) \quad (24)$$

the correspondent effective potential is:

$$V_{\text{eff}}(\zeta;\varepsilon,0,p_2)=\zeta^3+\varepsilon\zeta^2-\zeta+p_2^2 \quad (25)$$

their critical points are:

$$\bar{\zeta}_{\substack{\max\\\min}}=-\frac{1}{3}\left[\varepsilon\pm\sqrt{\varepsilon^2+3}\right] \quad (26)$$

with their corresponding energies:

$$\varepsilon_{\substack{\max\\\min}}=\frac{1}{27}\left[27p_2^2+9\varepsilon+2\varepsilon^3\pm(6+2\varepsilon^2)\sqrt{3+\varepsilon^2}\right] \quad (27)$$

The ζ-dependence of V_{eff} [see Equation (25)] for this mode, in Figure-3, is plotted. The solid color lines show the behavior for:$\varepsilon = 1.5$(green), $\varepsilon = 1$(blue), $\varepsilon = -0.5$ (red), and $\varepsilon = -1$ (black) The initial conditions to describe this mode are $p_1 = 0$, and $p_2 = 0.01$. The dotted vertical blue line is the projection on the ζ-axis,and the dotted horizontal blue line is on the potential(evaluated

at $\varepsilon = 1$), where the maximum critical point ($\bar{\zeta}_{\max}$) is observed[see Equation (26)]. A similar description for the dotted vertical/horizontal blacklines is done for the minimum critical point ($\bar{\zeta}_{\min}$) at $\varepsilon = -1$.

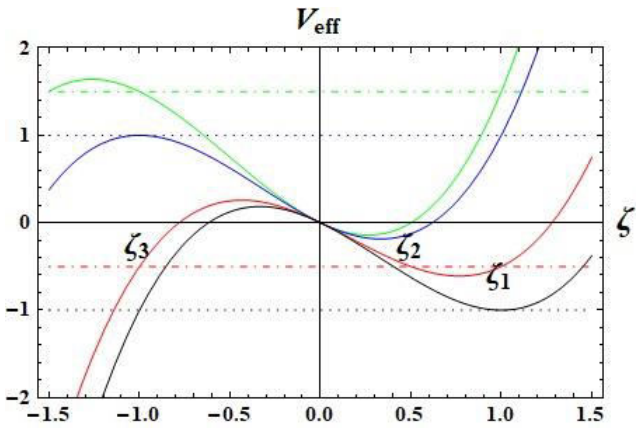

Figure-3. ζ-dependence of V_{eff} for plane mode. The colored lines represent the behavior for the following conditions: $\varepsilon = 1.5$ (solid green line), $\varepsilon = 1$ (solid blue line), $\varepsilon = -0.5$ (solid red line), and $\varepsilon = -1$ (solid black line). The initial conditions are $\varepsilon = 0.4$, $p_1 = 1$and $p_2 = 1$.

The horizontal red short dashed line intercepts the solid red line at three points, and only $\zeta_1$and ζ_2, localized on the concave up curve, are the turning points.

A bounded oscillatory motion is obtained with these initial conditions and reduced energies in the interval$-1 < \varepsilon < 1$. At$\varepsilon = 1$, the pendulum is in its highest position, corresponding to the value $\bar{\zeta}_{\max} = -1$, and for $\varepsilon = -1$, in its lowest position ($\bar{\zeta}_{\max} = 1$).For anε-value greater than 1, for example$\varepsilon = 1.5$ (green line), the motion has not turned points as is showed by the horizontal green short-dashed line, in this case, the pendulum is restricted to be move in the finite interval$-1 < \zeta < 1$ or the pendulum has a bounded motion.

Figure-4 displays the temporal derivative ofζas a function of ζor phase diagram to visualize the dynamics of the plane mode. One point in this plane gives a well-defined system state. Therefore, the curve for $\varepsilon = -1$is the only one that does not pass through the point (1, 0) becauseζ has a value of one ($\bar{\zeta}_{\min} = 1$ indicates that the pendulum is in its lowest position or the pendulum is hanging in that position).

For $\varepsilon = -0.5$ (red curve), the pendulum has an oscillatory motion (the trajectory, as the closed curve, is illustrated) between $\zeta_1$and ζ_2 at the interval $0.5 < \zeta < 1$.For the blue curve ($\varepsilon = 1$), ζ has a value of minus one ($\bar{\zeta}_{\max}$indicates that the pendulum is in the highest position), and its unstable equilibrium position (any slightest disturbance makes the pendulum fall) is at $(-1, 0)$or bifurcation point.

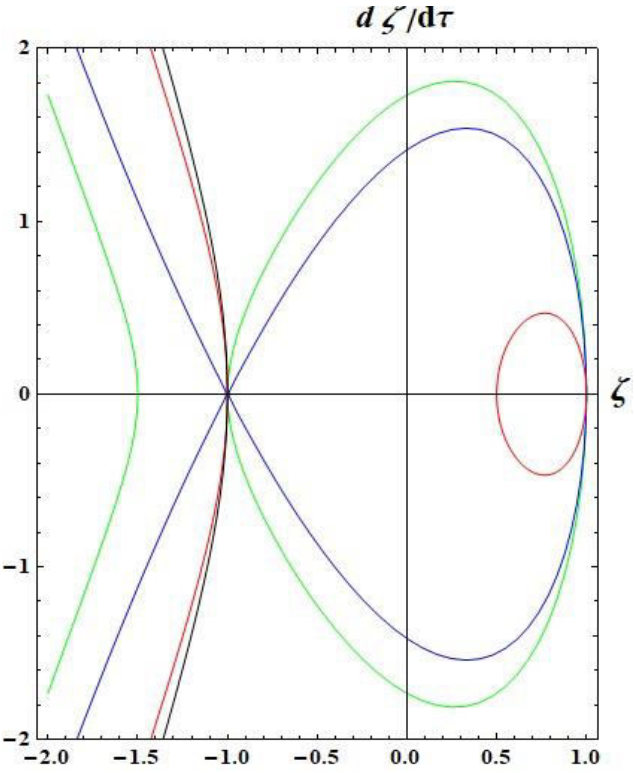

Figure-4. ζ-dependence of $d\zeta/dt$ or phase diagram for plane mode for some reduced energy values: the green line is for $\varepsilon = -1.5$, the blue line for $\varepsilon = 1.0$, the red line is for $\varepsilon = -0.5$, and the black line for $\varepsilon = -1$ (here $p_1 = 0$, and $p_2 = 0.01$). All curves pass through the point (1, 0).

The representation of the unphysical solution is given by the green curve or$\varepsilon = 1.5$. In this case, the pendulum has a bounded motion for$-1 < \zeta < 1$.

Conical Mode

The effective potential that characterizes this mode reduces to $V_{\text{eff}}(\zeta_s; \varepsilon, p_1, p_2) = \varepsilon_{\min}$. Since the CM of PSP describes a uniform circular motion on a horizontal plane at a fixed height, Equation (13) is factorable in linear and quadratic factors. The two roots of the quadratic term are equal and correspond to the height at which the mass describes its circular path, while the third root (linear factor) is the unphysical solution.
The characteristics of conical mode are:

$$\dot{\phi}(\tau) = \text{const} \tag{28}$$

$$\zeta(\tau) = \bar{\zeta}_{\min} = -\frac{1}{3}\left[\varepsilon - \sqrt{\varepsilon^2 + 3(1 + p_1)}\right] \tag{29}$$

where $\tau = \Omega_0 t$ and $\Omega_0 = \sqrt{\frac{mg\ell}{I_{\bar{x}}}}$. For $\bar{\zeta}(\tau)$ constant and defining

$$\bar{\zeta}(\tau) = \zeta_s, \ \forall\tau \tag{30}$$

$$\dot{\phi}(\tau) = \dot{\phi}_s, \ \forall\tau \tag{31}$$

Integrating Equation (31):

$$\phi(\tau) = \dot{\phi}_s \tau + \phi_0 \tag{32}$$

with ϕ_0 some constant.

Otherwise, the spin motion also remains constant, Equation (7) becomes:

$$\dot{\psi}_s = \frac{p_\psi}{I_{\bar{z}}} - \dot{\phi}_s \zeta_s \tag{33}$$

Integrating$\dot{\psi}_s$

$$\psi_s = \dot{\psi}_s \tau + \psi_0 \tag{34}$$

$\psi_0$is another constant. Equations (29) − (34) are to solve this mode.

The reduced energy ε for this mode as a function of height ζ_s is

$$\varepsilon = \frac{1}{2\zeta_s}\left[1 + P_\phi P_\psi + P_\psi^2\, \zeta_s(\alpha - 1) - 3\zeta_s^2\right] \tag{35}$$

where P_ϕ and P_ψ are constants.

Figure-5 shows the behavior of $V_{\text{eff}}\,(\zeta, p_1, p_2)$in the range from $-2$to 1.5 for the conical mode with initial conditions $\varepsilon = 0.8909,\ p_1 = 0.6409,$ and$p_2 = 1.1677.$ $\zeta_s$means a height independent of time.

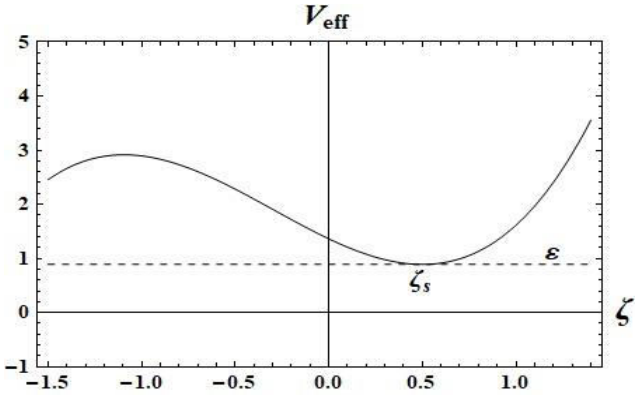

Figure-5. Behavior of effective potential as a function of ζ for the conical mode. The initial conditions are $\varepsilon = 0.8909, p_1 = 0.6409,$ and $p_2 = 1.1677.$

There are two frequencies associated with the same height and spin motion:

$$\Phi_+ = \frac{P_\psi + \sqrt{P_\psi^2 + 4\zeta_s}}{2\zeta_s} \tag{36}$$

$$\Phi_- = \frac{P_\psi - \sqrt{P_\psi^2 + 4\zeta_s}}{2\zeta_s} \tag{37}$$

with$\Phi_+ > \Phi_-$. Equation (36) represents counterclockwise frequency (as precession) and Equation (37) is clockwise direction (slow precession).

There are two conical modes associated with both the same height $\zeta_s$and the spin angular momentum$P_\psi$the first, associated with the orbital angular momentumP_ϕ with frequency$\Phi_+$and, the second, Φ_-. The difference between the two modes lies in the orbital and spin angular frequencies that describe the CM circular trajectories.

The spin motion, or how the pendulum is rotating, in dimensionless units, is given by:

$$\Psi_s = \frac{\dot{\psi}_s}{\Omega_0} = \frac{1}{2}\left[P_{\psi s}(2\alpha - 1) \pm \sqrt{P_{\psi s}^2 + 4\zeta_s}\right] \tag{38}$$

The phase diagram for this mode, for $\zeta_s = \zeta/\ell$, in Figure-6 is plotted. An energy $\varepsilon = 9/8$and an orbital angular momentum$P_\phi = 7/4$ are required to obtain a spin angular momentum $P_\psi = 0.5$. The region of interest is around point (0.5,0 or the interval $0.476 < \zeta < 0.544$.

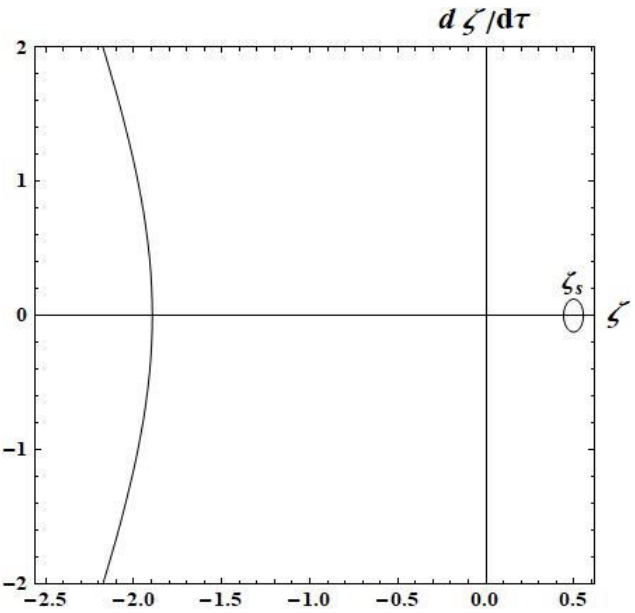

Figure-6. Phase diagram for the conical mode. The conditions are $\varepsilon = 0.8909, p_1 = 0.6409,$ and $p_2 = 1.1677.$

Elliptical Mode

In this mode, the CM of the pendulum moves between two horizontal planes $\zeta = \zeta_i$ (ζ_i are the turning points, i = 1, 2). The characteristics of elliptical mode are:

$$p_1 \neq 0, \qquad -1 \leq p_1 \leq 2 \qquad \frac{1}{2}(p_1 - 2) \leq \varepsilon \tag{39}$$

involving the physical condition:

$$\zeta_3 < -1 \leq \zeta_2 < \zeta_1 < 1 \tag{40}$$

In Figure-7, the behavior of V_{eff} as a function of ζ is displayed. The turning points $\zeta_3 < \zeta_2 < \zeta_1$ are shown on the horizontal axis, and the motion is bounded and the physical interest for $-1 < \zeta_2 < \zeta < \zeta_1 < 1$. For this

elliptical mode, $-1.5 < \zeta < 1.2$is the range with initial conditions $\varepsilon = 0.6, p_1 = 4.0 \times 10^{-6}$ and $p_2 = 0.3625$.

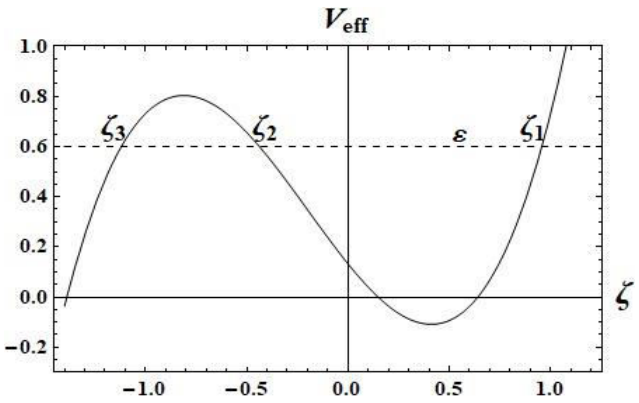

Figure-7. ζ-dependence of V_{eff} for elliptical mode with initial conditions $\varepsilon = 0.6, p_1 = 4 \times 10^{-6}$, and $p_2 = 0.3625$.

The corresponding phase space is sketched in Figure-8. There are three roots of which$\zeta_1$and $\zeta_2$are physical solutions, and ζ_3 violates the ligature. The periodic motion is bounded, and the condition $\zeta_2 < \zeta < \zeta_1$ is fulfilled, as shown in Figure-7.

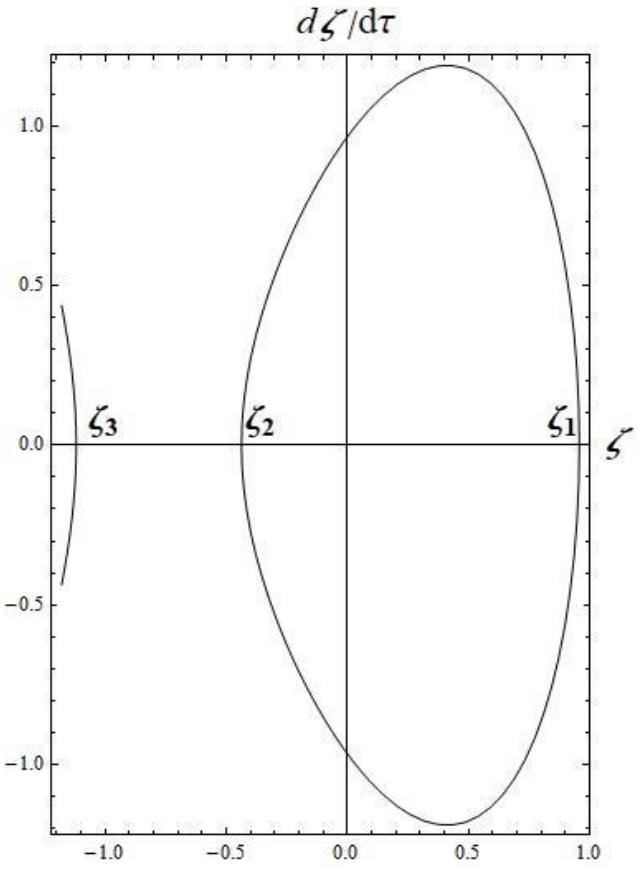

Figure-8. Phase diagram for the elliptical mode. The conditions are $\varepsilon = 0.6, p_1 = 4 \times 10^{-6}$, and $p_2 = 0.3625$.

CONCLUSIONS

By using the techniques of variation of canonical variables, based on the Lagrangian formalism, the effective potential is deduced which has a dependence on one variable (ζ) related implicit with nutation angle θand three fitting parameters reduced energy (ε) and two reduced angular momenta (p_1 and p_2).

The asymmetric behavior of effective potential as a function of ζvaries for the three modes (plane, conical, and elliptical) mode for the ζ-range, but the behavior is similar.

The phase diagram shown that in the plane mode, the motion is on a plane, for the conical mode, it vibrates at a single point and in the elliptical mode, it moves quasi elliptical and these motions depends on the initial condition.

An advantage of this approach was to obtain approximate analytical expressions to study the phase diagrams for these three modes.

REFERENCES

[1] Giltinan D. A., Wagner D. L. and Walkiewicz T. A. 1996. The physical pendulum on a cylindrical support. Am. J. Phys. 64: 144-146.

[2] Suzuki M. and Suzuki I. 2008. Physics of simple pendulum a case study of non-linear dynamics. [Online]. Available: https://www.researchgate.net/ publication/332766499.

[3] Braginsky V. B., Polnarev A. G. and Thorne K. S. 1984. Foucault pendulum at the South Pole: proposal for an experiment to detect the Earth's general relativistic gravitomagnetic field. Phys. Rev. Lett. 53: 863-866.

[4] Butikov E. I. 1999. The rigid pendulum - an antique but evergreen physical model. Eur. J. Phys. 20: 429-441.

[5] Baker G. L. and Blackburn J. A. 2005. The Pendulum: A case study in Physics. Oxford University Press, New York.

[6] Matthews M. R., Gauld C. F. and Stinner A. (Editors) 2005. The pendulum, historical, philosophical and educational perspectives. Springer, Netherlands.

[7] Chernyavsky A. and Pelinovsky D. E. 2016. Breathers in Hamiltonian PT-symmetric chains of coupled pendula under a resonant periodic force. Symmetry. 8: 59-86.

[8] Manevitch L. I., Smirnov V. V. and Romeo F. 2016. Stationary and non-stationary resonance dynamics of

the finite chain of weakly coupled pendula. Cybern. Phys. 5: 130-135.

[9] Prichani J. S., Sakwa T. W. and Ongati N. O. 2017. Functions of multi-pendula system in spatial motion. The Standard International Journal (The SIJ) ISSN 2321-2381, 5: 1-5.

[10] Salerno G., Berardo A., Ozawa T., Price H. M., Taxis L., Pugno N. M. and Carusotto I. 2017. Spin-orbit coupling in a hexagonal ring of pendula. New J. Phys. 19: 055001/1-16.

[11] Fernandes J. C., Sebastião P. J., Gonçalves L. N. and Ferraz A. 2017. Study of large-angle anharmonic oscillations of a physical pendulum using an acceleration sensor. Eur. J. Phys. 38: 045 004/1-18.

[12] Bhadra N. 2018. Dynamics of a system of coupled inverted pendula with vertical forcing, arXiv:1803.01643 [physics.class-ph]: 1-15.

[13] Singh P., Singh R. C. and Singh M. 2018. Study of normal modes and symmetry breaking in a two-dimensional pendulum, arXiv: 1806.06222 [physics.class-ph]: 1-15.

[14] Boubaker O. and Iriarte R. (Editors) 2018. The inverted pendulum in control theory and robotics. From theory to new innovations. The Institution of Engineering and Technology, London.

[15] Ndikilar C. E., Saleh A. I., Hafeez H. Y. and Taura L. S. 2019. Analytical calculation of power flow between two weakly coupled pendula and its application to an optical switch. Int. J. Theor. Math. Phys. 9: 25-35.

[16] Andrianov I. V., Manevich A. I., Mikhlin Y. V. and Gendelman O. V. (Editors) 2019. Problems of Nonlinear Mechanics and Physics of Materials. Springer International Publishing AG., Switzerland.

[17] Barone A. F., Acernese F. and Giordano G. 2019. Method for the measurement of angular and/or linear displacements utilizing one or more folded pendula, August22, Us Patent Application 2019/0257653A1. [Online]. Available: https://patents.google.com/patent/US20190257653A1/en.

[18] Pramreiter M., Stadlmann A., Linkeseder F., Keckes J. and Müller U. 2020. Non-destructive testing of thin birch (betula pendula roth) veneers. Bio Res. 15: 1265-1281.

[19] Trocaru S., Berlic C., Miron C. and Barna V. 2020. Using tracker as video analysis and augmented reality tool for investigation of the oscillations for coupled pendula. Roman. Repor. Phys. 72: 902-1/16.

[20] Finn J. M. 2008. Classical Mechanics. Massachusetts: Infinity Science Press LLC.

[21] Piña E. 1993. On the motion of the symmetric Lagrange's top. Rev. Mex. Fís. 39: 10-31.

[22] MacMillan, W. D. 1960. Dynamics of rigid bodies, Dover Publications.

[23] Provatidis, C. G. 2012. Revisiting the Spinning Top. Int. J. Mat. Mech. Engin. 1: 71-88.

[24] Klein F., Sommerfeld A. 2010. The theory of the Top, Volume II (Birkhaüser, Boston).

[25] Maya H., Diaz R. A. and Herrera W. J. 2015. Study of the apsidal precession of the physical symmetrical pendulum. J. Appl. Mech. 82: 021 008/1-12

[26] Taylor J R. 2005. Classical Mechanics (Dulles: University Science Books).

[27] Lagrange J. L. 1997. Analytical Mechanics, Translated from the Mécanique analytique, novelleédition of 1811. Springer-Science+Business Media, B.V., Netherlands.

[28] Awrejcewicz J. 2012. Classical Mechanics. Springer, New York.